Calculation and Measurement of Winding Loss at High-Frequency Pulsed Currents

A. Pokryvailo and H. Dave
Spellman High Voltage Electronics Corporation, Hauppauge, NY 11788 USA
apokryva@spellmanhv.com

***Abstract*— Rich literature exists on calculation of copper loss in windings of high-frequency transformers and inductors. Most of the work was carried out in a Dowell approximation ignoring the windings aspect ratio and core presence. Calculation of losses at non-sinusoidal currents is made usually by summing the harmonics losses. This paper makes an example of an inductor with an open ferromagnetic core and a high winding aspect ratio. Simulations were performed on a COMSOL platform, both in frequency and time domains. The latter enable avoiding drudge and inaccuracy of harmonics approximation in the case of periodic signals and give possibility of calculating losses at arbitrary-shaped currents. The advantages of time-domain approach are distinct when the winding is driven by pulsed current with a low duty cycle D. Methods and simulation results are provided for pulsed sine, rectangular, triangular, and arbitrary shapes at different D's. First, benchmarking was performed by comparing simulations in the frequency- and time-domains at purely sine waves. It was found that in both simulations the results were very close to each other, and from that, we proceeded to pulsed excitation. It was found that losses at pulsed sine waves were much higher than were those calculated in the frequency domain by summing the losses from up to 11 first harmonics. The rectangular waves generated the highest losses, up to tenfold of those at sine wave. It was also found that the ferromagnetic core increases the loss considerably compared to the case of an air-core inductor, which was confirmed experimentally. The windings resistance was measured with an LCR meter in a wide range of frequencies, up to 1MHz. In addition, adiabatic heating experiments were conducted with the winding driven by DC (for power calibration), sine, and pulsed quasi-sine waves at different frequencies and D's. The experimental results were found in fair agreement with their theoretical counterparts.**

Keywords—power losses, pulsed current, skin effect, proximity effect, COMSOL

I. Introduction

It is well known that the winding resistance increases manifold at high frequency (HF). In multilayer windings, the increase is mainly due to proximity effect. The practical impact of this phenomenon has grown tremendously with the advance of power electronics. Papers on calculation of ac resistance count in many hundreds if not thousands; there are a few on the *experimental* verification of the theoretical results. As early as in 1989, there was felt a need in a systematization of the existing literature [1]. Since then, many more publications have appeared, some of them making use of numerical field analysis. Most of the work was carried out in a Dowell approximation [2], ignoring the windings aspect ratio and core presence. The analysis that had started with sine waves has been extended to the case of non-sinusoidal currents, mostly made with the help of Fourier series by summing losses from several harmonics (see, e.g., [3], [4], and references of [1]). It has also been recognized that the core and external objects can considerably increase copper losses [5]. Another factor compromising the accuracy of analytical approaches is the winding build, especially for the windings with high aspect ratio and curvature. In the latter cases, field simulations are most appropriate.

This paper makes use of an inductor with an open ferromagnetic core, large winding curvature, and a high winding aspect ratio as a case difficult for analytical analysis. The winding losses were both calculated and measured for a wide range of frequencies and a variety of current waveforms. Simulations were performed on a COMSOL platform, both in the frequency domain (FD) and time domain (TD). The latter abolish drudge and inaccuracy of the harmonics' approximation in the case of periodic signals and give possibility of calculating losses at arbitrary-shaped currents, not necessarily periodic ones. Understandably, some generality is lost, but many important insights are gained. It is argued that the TD simulations are a useful complement to analytical methods in the case of low duty cycle currents and may vie for their replacement owing to a wide deployment of field simulation packages in industry.

II. Theoretical

As a physical object, the inductor investigated in this report has 140 turns of magnet wire AWG#26 wound in five layers on an 8-mm-diameter, 38-mm-long ferrite slug (dc resistance R_{dc}=0.75 Ω, inductance L=0.9 mH at 60 kHz; other designs have also been investigated but not reported here). Its structure, in relevant detail, is shown in Figure 1 as the geometry of a simulation model. (Actually, only half of the space was modeled owing to the symmetry in the midplane.) Each individual wire has a fine mesh with boundary layers adaptable to the simulation frequency f_s=1/T_s (or the higher harmonics in the case of TD simulation). The core is modeled as a ferromagnetic object with a constant relative permeability μ_r=1000 if not stated otherwise. Core loss calculation has also

been performed but is omitted as being out of the scope of this paper. We only note upfront that copper losses dominate.

Current waveforms can be quite complex. Typically, the current pulses have a bipolar pulsed shape with duration $\tau < T_s/2$ (duty cycle D= $\tau/T_s/2$); unipolar currents are also common. In some electronic circuits, e.g., rectifiers/voltage multipliers, currents can be asymmetric; the latter factor is ignored below.

All simulations were performed with Magnetic Fields interface; loss integration in TD was done with Global ODEs and DAEs interface. "Events" were used to save computational resources at low *D*: time steps were small only on Events, namely, during pulsed current excitation.

A. AC resistance Rac - FD

1) Sine waveforms

FD simulations are simple; they are given here only as a baseline for the main content, namely TD simulations. Normalized calculated ac resistance Rac/Rdc is plotted in Figure 2 along with its experimental counterpart (measured with a Precision Quadtech LCR meter, model 1920), and Dowell approximation ([2], Eq. (10)). There is a fair correspondence of the simulated and measured data. The measured values include also the core and dielectric losses; both should be negligible at the low drive power of the instrument. There is high confidence in both the simulations and measurements: there are no significant non-linearities nor unknown physics involved; copper properties are well known.

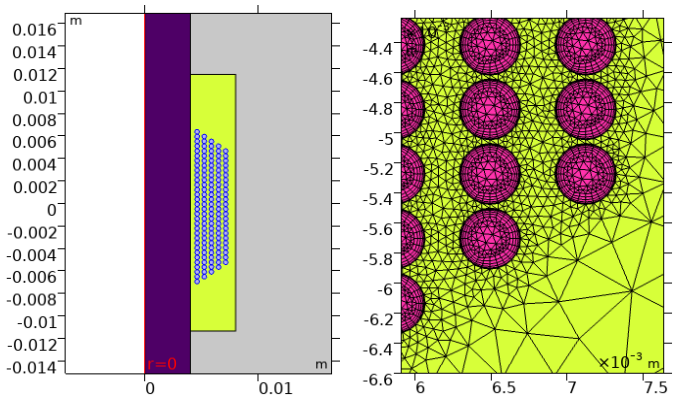

Figure 1. Modeled geometry (axisymmetric approximation) and mesh (adaptable to skin depth). Yellow shows winding encapsulation (was needed for calculation of parasitic capacitance and thermal simulations, omitted in this paper).

In the majority of the publications, the impact of the eddy currents (skin/proximity effects) on the increase of the copper losses is analyzed without accounting for the ferromagnetic parts. Intuitively, the core presence should enhance the field and increase the loss, at least, in a part of the winding. An identical winding, but on a dielectric former, was made to quantify the difference experimentally. It is illustrated by Figure 3, Figure 4. Note strong field at the outer turns for μ_r=1000. The simulation and experimental results match fairly well.

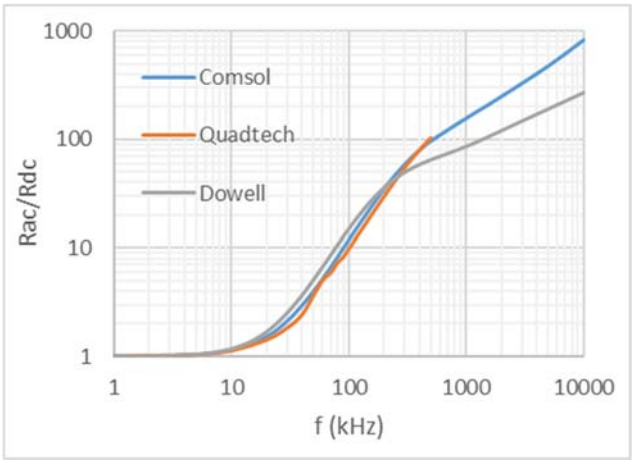

Figure 2. Frequency dependence of normalized inductor resistance.

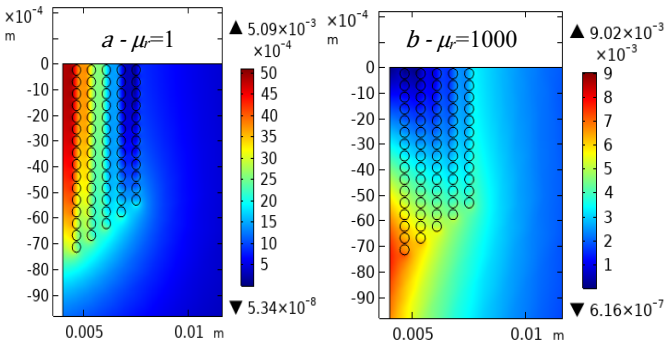

Figure 3. Magnetic flux density, T, in the winding for μ_r=1 and μ_r=1000 (60 kHz, peak current I_m=0.465 A).

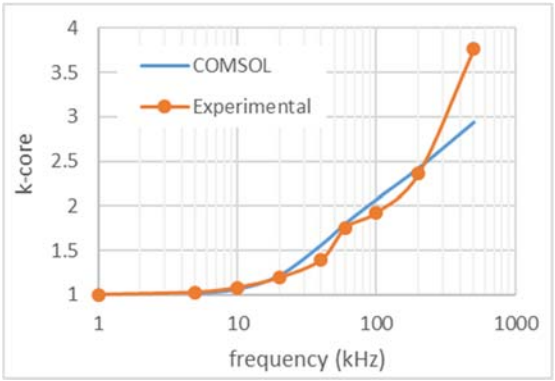

Figure 4. Core influence on winding losses in FD. k-core is ratio of ac resistance of winding on ferrite slug, R_{fer}, to that of winding on non-ferromagnetic (insulator) former, R_{ins}: k-core= R_{fer}/R_{ins}.

2) Pulsed sine waveforms

Consider, as an example, a pulsed sine waveform defined by the series

$$v(t,D) := \frac{4 \cdot D \cdot I_0}{\pi} \cdot \sum_k \left[\left(\frac{\cos(k \cdot \pi \cdot D \cdot 0.5)}{1 - k^2 \cdot D^2} \right) \cdot \cos(k \cdot \omega \cdot t) \right] \qquad (1)$$

where k=1, 3,…, N, and D is duty cycle. Plots of (1) for D=0.2, 0.25, 0.5 are shown in Figure 5a-c, calculated for 101 and 7 first harmonics, respectively. It is seen that seven harmonics are sufficient to approximate the pulsed wave at D=0.5 but are marginal for D=0.2. The total loss can be calculated by summing the losses from several harmonics. Paper [6], by treating the problem in TD, gave a *direct* proof of the validity this method (at least, for the case of a straight conducting cylinder).

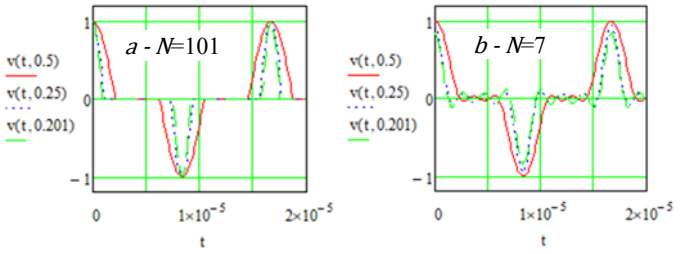

Figure 5. Plots of (1) for D=0.5, 0.25, and 0.201 (D=0.2 is a singular point) for N=101, N=7. f_s=60 kHz

B. *Copper losses - TD simulations*

The goal of TD simulations is finding the loss *directly* in a winding driven by an *arbitrary* waveform. It could be a periodic waveform, which is the most important case for power electronics, or anything else. The practical importance is in that a) experimentation is not easy with HF, high-power non-sine waveforms; b) the winding can be driven by simulated or experimental current waveforms, so the simulation can yield "true" results.

The same mesh was used for both FD and TD simulations. In TD, the winding was driven for several periods by either sine (for the direct comparison to FD simulations) or non-sine waveforms.

To validate TD simulations, several variables were computed for a number of frequencies in both FD and TD for a *sine* current with the *same* amplitude I_m=0.465 A, by the same procedure. A comparison of these variables, including the copper losses, showed that the TD simulation was set correctly.

1) Excitation function approximated by Fourier series - half-sine wave pulsed excitation

Pulsed sine waveforms were composed from 11 harmonics using (1) with some damping for better convergence. Sample waveforms are shown in Figure 6 (see also Figure 5). The winding loss was calculated as

$$P_w = \frac{1}{T_s} \int_{nT_s}^{(n+1)T_s} Qrh * dt, \qquad (2)$$

where n can be any integer, and *Qrh*='resistive losses' is a COMSOL variable. The simulation was run up to 5T_s (n=4), but it became clear that two periods were sufficient for attaining good accuracy. Thus, in all the results below, n=1 if not stated otherwise.

The current through a strand (computed by integration of the current density phi-component, *Jphi*, over the wire cross-section) for several D's is shown in Figure 6. It is seen that even 11 harmonics do not bring the current amplitude to 0.465 A at small D's. A comparison of losses at sine wave, *Psine*, to losses *Psine(D)* at pulsed wave is shown in Table 1 for several frequencies. The results were close to those found by summation of losses from several harmonics in FD, which promoted confidence in TD simulation for such coils. Yet, it became evident that the Fourier series does not work well for small D's.

2) Excitation function inputted directly

Yet the next step was forgoing the Fourier series in favor of "drawing" a pulsed function directly (realized by specifying a piecewise function in COMSOL for idealized waveforms). This resolves the problem of approximation at small D's, where a large number of harmonics needs to be called for; it also makes easy excitation by arbitrary waveforms.

Table 1. Comparison of losses at sine wave, *Psine*, to losses *Psine(D)* at pulsed sine wave, for several frequencies.

f_s (kHz)	*Psine(D)/Psine*			
	D=0.99	D=0.5	D=0.25	D=0.201
40	0.980	1.190	1.553	1.631
60	0.981	1.201	1.433	1.444
200	0.974	0.772	0.641	0.594

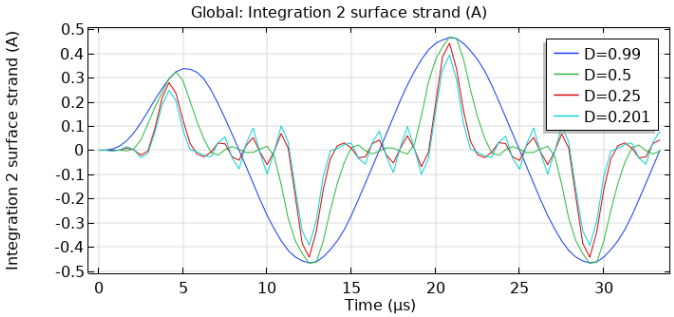

Figure 6. Current through the wire (computed by integration of *Jphi* over cross-section).

a) Half-sine wave pulsed excitation (D<1)

A summary graph of the ratio of losses at excitation by a pulsed half-sine wave (D<1; see an example Figure 7) to those at a sine wave (D=1), P_{pulsed}/P_{sine}, is shown in Figure 8. For this specific inductor, the said ratio peaks up to ≈1.8 at 40-60 kHz and D=0.1-0.2, which is much higher than that determined in both FD and TD simulations based on Fourier series for small D's. This is explained by the disregard of high harmonics in waveforms composed by (1). Note that at very low f_s, P_{pulsed}/P_{sine} tends to D. Obviously, this happens because the heating is proportional to the rms value: eddy currents are insignificant. There is a similar tendency at very high f_s:

skin/proximity effects are so strong that the current is concentrated on the wire perimeter anyway. The total loss grows as $\sqrt{fs}$ (by f_s, high harmonics are also meant here), but is proportional to I^2, as seen from the following formula for the loss, P_{skin}, at strong skin effect [7]

$$P_{skin} := \sqrt{\frac{2\cdot\pi\cdot f_s\cdot\mu_0\cdot\mu_r}{2\gamma}}\cdot\frac{H^2}{2}$$

where γ is copper conductivity, μ_0 is vacuum permeability, and H is magnetic field that is proportional to the current.

b) Rectangular pulsed excitation (PWM square wave)

One would expect, intuitively, that owing mainly to a larger harmonic content, a rectangular wave (see an example Figure 9) would produce higher losses compared to a half-sine wave pulsed excitation with the same D. According to the simulation results, this is indeed the case, as seen from Figure 10. It appears that sharp transitions are conducive to a very steep rise in loss, tenfold at 20-40 kHz; higher rms value is secondary.

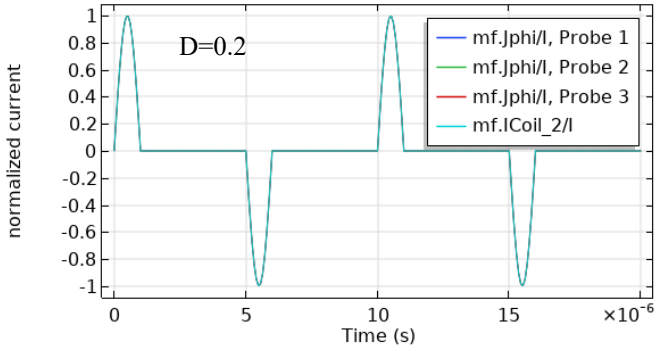

Figure 7. Pulsed sine inductor current at D=0.2, 100 kHz. Three first legends are currents through three different strands (computed by integration of *Jphi* over cross-section), fourth is excitation, all normalized to amplitude. Note that all traces are indistinguishable, which is evidence of high accuracy.

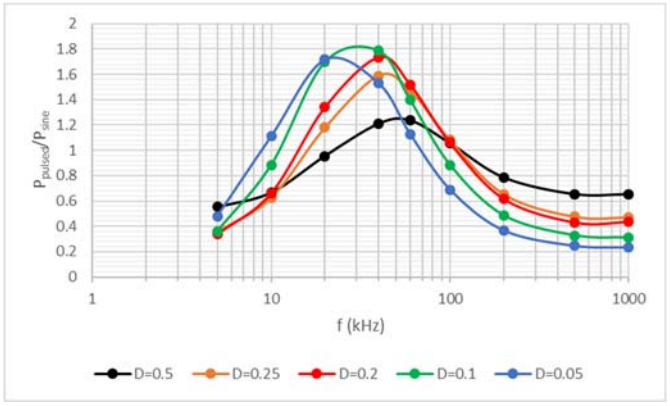

Figure 8. Frequency dependence of the ratio of losses P_{pulsed}/P_{sine} at pulsed excitation by a half-sine wave (D<1) to those at sine wave (D=1). $P_{pulsed} \equiv P_{sine}(D)$.

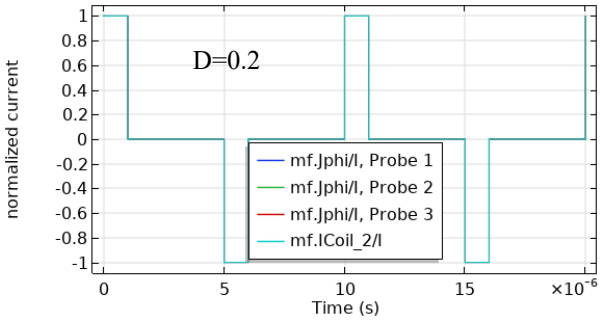

Figure 9. Winding excited by pulsed rectangular wave (D=0.2). See legends' explanation in Figure 7.

Square waves are, probably, an idealized case, not encountered in practice at HF; the transitions are smoothed by natural reasons.

c) Triangular wave pulsed excitation (D<1)

By a similar logic, one would expect that a triangular wave (see an example in Figure 11) would induce lower losses than a rectangular one. A frequency dependence of the ratios of losses $P_{triang}(D)/P_{sine}$ and $P_{triang}(D)/P_{sine}(D)$ at pulsed excitation by a triangular PWM wave for several D's shown in Figure 12 is in line with this intuitive thinking. In fact, in most combinations, the losses at sine wave are higher than at triangular ones, the exception being the frequency range of ~20-70 kHz. At pulsed excitation, the pulsed sine wave invariably generates higher losses than its triangular counterpart does.

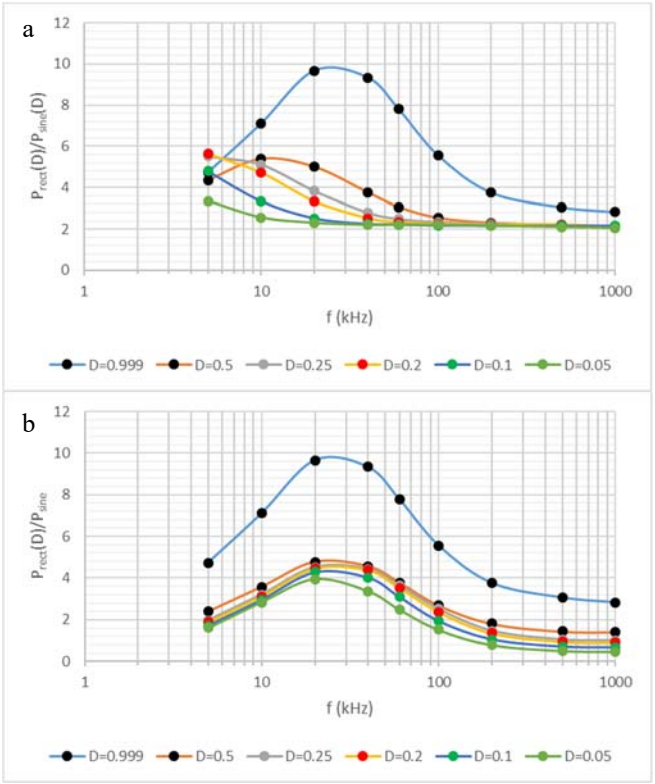

Figure 10. Frequency dependence of the ratio of losses $P_{rect}(D)/P_{sine}$ and $P_{rect}(D)/P_{sine}(D)$ at pulsed excitation by a rectangular PWM wave (D<1).

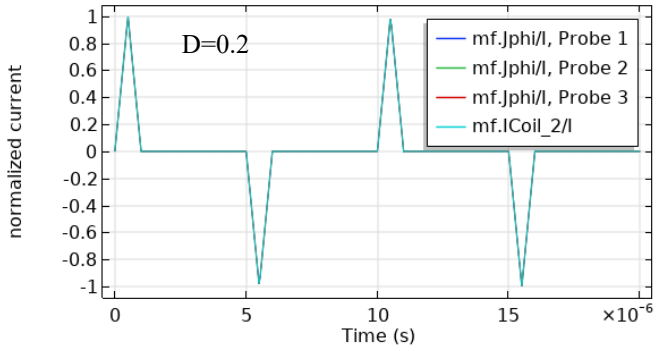

Figure 11. Winding excited by pulsed triangular wave (*D*=0.2). See legends' explanation in Figure 7.

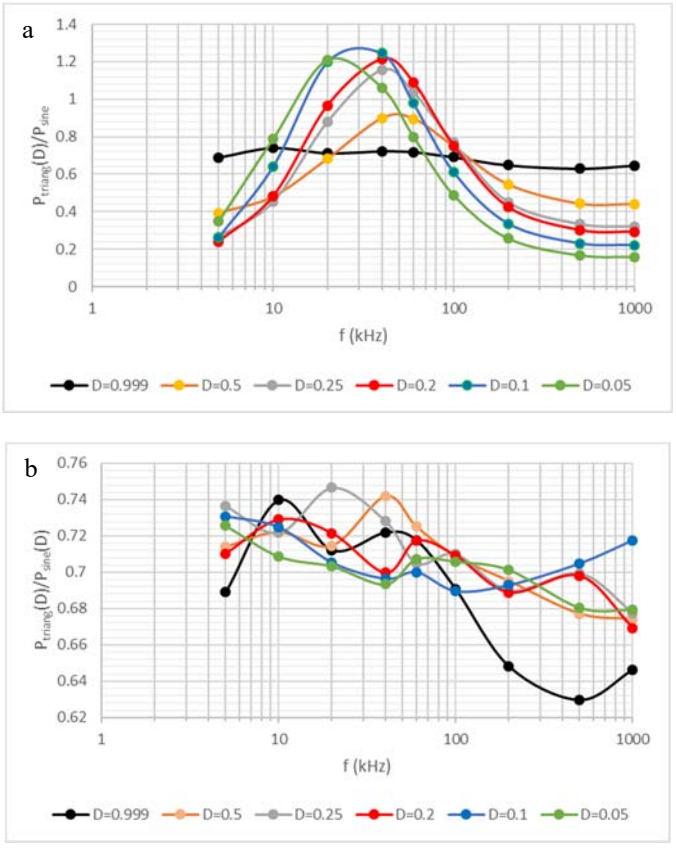

Figure 12. Frequency dependence of the ratio of losses $P_{triang}(D)/P_{sine}$ and $P_{triang}(D)/P_{sine}(D)$ at pulsed excitation by a triangular PWM wave (*D*<1).

d) Arbitrary wave excitation

COMSOL allows importing waveforms from other applications (e.g., experimental waveforms from a digital scope, PSpice waveforms, etc.; txt and csv formats are most convenient). Special care should be taken to denoise the waveforms by removing frequencies of no interest, especially bit fluctuations. Otherwise, the simulator follows all insignificant variations, and simulation time becomes unreasonably long without bringing any additional value.

Figure 13 shows an example of simulation with the driving current reproducing the experimental waveform Figure 14. Experimental methods and results of this particular simulation will be discussed in the next Section.

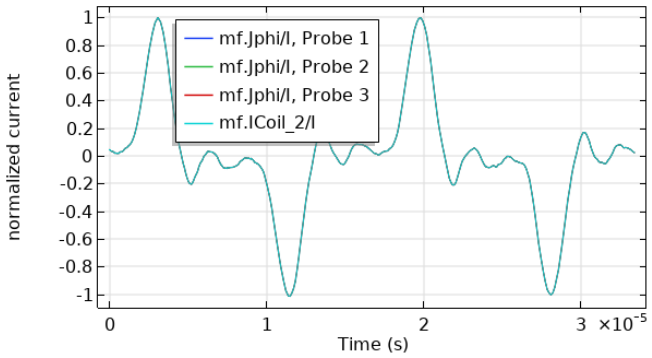

Figure 13. Winding excited by pulsed "sine" wave (*D*≈0.4) Figure 14. See legends' explanation in Figure 7.

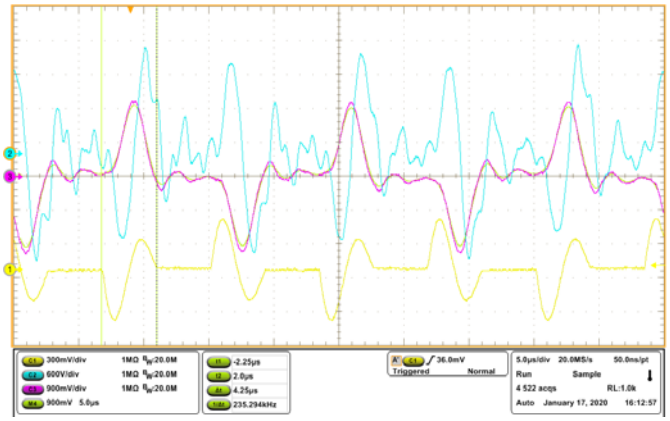

Figure 14. Experimental waveforms in one of the adiabatic heating experiments. Ch1=Power Amplifier input); Ch2=inductor voltage, 600 V/div; Ch3=inductor current, 0.9 A/div, Pearson 2877 (pink). Horizontal 5 μs/div. 60 kHz.

III. Experimental - Adiabatic Heating

Experimental determination of losses at arbitrary HF currents and high ratio of L/R is difficult on several counts. First, there is the power generation aspect. A common way of generating high HF current is amplifying the desired waveform with an RF power amplifier (PA). Since an inductance current is an integral of the applied voltage, the input waveform should be a derivative of the desired current. A real inductor requires more tailoring—as an example, see the PA input, ch1, Figure 14. The necessity to operate at HV does not help. The inductor voltage can be estimated as $V = 2\pi f_s LI$. For the inductor in question, at I=2 A, fs=200 kHz, V=2.26 kV (compare to the blue trace ch2 Figure 14). Thus, a wide-band matching transformer is mandatory for most PAs (we used a 1 kW, 20 kHz-400 kHz PA, model 1000S04 by Electronics & Innovation; the matching transformer was workshop-made).

Second, accurate electrical measurement of losses at several watts is problematic because the reactive power is three orders of magnitude higher. This is why we opted for thermal methods, namely adiabatic heating, where heating curves at unknown power generated by an arbitrary mechanism can be compared to calibration curves obtained at a known power. Alternatively, certain scenario, e.g., heating by sine wave, can serve as a baseline, and other scenarios can be judged against it.

An impregnated inductor was thermally insulated with a thick foam plastic. One thermocouple was placed on top of the winding, another attached to the core, close to the winding. First, calibration runs were made with a DC power supply. It became clear that thermal insulation was far from ideal, so low power heating, below ≈5 W, deviated strongly from the adiabatic one. The inductor heat capacity derived from both the experiment and COMSOL simulations is C_p≈25 J/K.

The inductor was heated by an approximately pulsed sine current with a *fixed* amplitude, at different f_s and D's, the latter varied from unity (sine wave), as the basis, down to approximately D=0.2. Lower D's were not realized because of an excessively high voltage needed to drive the inductor. Heat insulation was identical for all runs. Because the waveforms are not "clean", D-values cited below (estimated for the inductor current, ch3) are rather approximate, if not arbitrary. Time was counted to heating from 40 °C to 80 °C; it is denoted as $t_{40\text{-}80}$. Absolute power can be conveniently estimated using C_p: $P = \frac{C_p \Delta T}{t_{40-80}}$, from which the winding resistance, neglecting core and insulation losses, is R_{ac}=2P/I_m^2. For an instance of the experiment Figure 15, sine wave, P=8 W, and R_{ac}=4 Ω, or R_{ac}≈5.3R_{dc} (compare to Figure 2).

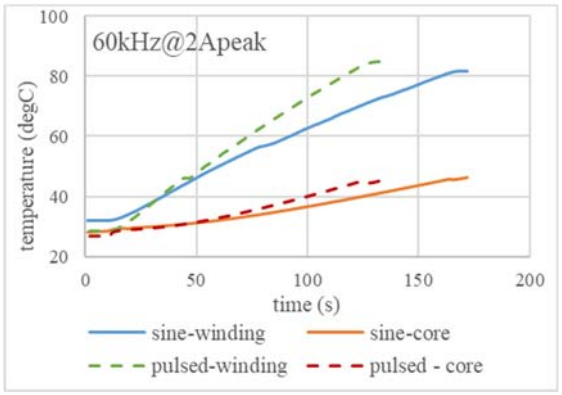

Figure 15. Adiabatic heating by current I_m=2 A at 60 kHz. Solid lines – sine wave, dotted lines – pulsed wave Figure 14.

Since the interval $t_{40\text{-}80}$ is inversely proportional to the loss (*assuming adiabatic process*), a higher-accuracy comparison can be made between power losses at different scenarios. As an example, power, in arbitrary units, is tabulated in Table 2 for 60 kHz, where the basis, P=1 au, is assigned to D=1. The subscripts "*exp*" and "*coms*" in Table 2 relate to the experimental and COMSOL data, respectively, whereas the latter are described in Sect. II.B.2)d) (the winding was driven by denoised experimental waveforms).

Table 2. Experimental data on inductor heating at 60 kHz compared with COMSOL simulations Sect. II.B.2)d) (in simulations, winding was driven by experimental waveforms).

I_m (A)	I_{rms} (A)	D	$t_{40\text{-}80}$ (s)	P_{exp} (au)	P_{coms} (au)	remark
1.5	1.045	1	263	1	1	
1.5	0.802	0.5	154	1.71	1.41	
1.5	0.596	0.3	180	1.46	1.45	
2	1.38	1	125	1	1	
2	0.798	0.3	83	1.5	1.36	Figure 14

It is seen that the pulsed current heats up the inductor faster than the corresponding sine wave does. The experimentally found loss increase is typically somewhat larger than that predicted theoretically for both the idealized pulsed sine waves (Table 1, Figure 8) and experimental waveforms. The discrepancy can be attributed to at least three factors: heating the surroundings (non-adiabatic heating), added core loss, and higher content of high harmonics compared to idealized waveforms. The first factor would dominate at low power. Indeed, if the losses were low enough, 80 °C would never be reached: the ratio P(au) would become infinity. It is important to note that in all tests, the wire was much hotter than the core; *winding losses dominated.*

This section illustrates the problem complexity, and difficulty of experimental investigation. If in doubt, there is a need of scrutiny, probably, not envisaged at lower frequencies.

IV. Conclusions

We have demonstrated convenience and power of TD simulations in the case of pulsed currents, above all, at low D, compared to summing losses for multiple harmonics. This method stands out if real, complex current waveforms are known. It was shown that at the same frequency and amplitude, pulsed currents induce usually much higher winding losses than sine currents. This effect is pronounced at pulsed sine, and especially square waves, being much mitigated at triangular shapes.

It was also shown that the core presence has strong influence on the magnetic field, increasing the losses manifold compared to an air-core design.

An experimental investigation comprised R_{ac} measurement with an LCR meter (sine wave, low power) and high-current adiabatic heating experiments with sine and pulsed waveforms. Both confirmed fair accuracy of the field simulations, and a significant loss increase at pulsed excitation. The developed methods were expanded to Litz-wound inductors. This work will be reported later.

V. Acknowledgement

The authors thank Dr. W. Frei of COMSOL Inc. for his valuable help in debugging and setting time integration procedures. They also acknowledge support of this work by Spellman High Voltage Electronics Corp.

REFERENCES

[1] G. R. Skutt, T. G. Wilson, A. M. Urling, and Van A. Niemela, "Characterizing high-frequency effects in transformer windings—a guide to several significant articles", 4th APEC Baltimore MD, 13-17 Mar. 1989, pp. 373-385.

[2] P.L. Dowell, "Effects of eddy currents in transformer windings", Proceedings of the IEE, vol. 113, no. 8, pp. 1387–1394, Aug. 1966.

[3] W. G. Hurley, E. Gath, and J. G. Breslin, "Optimizing the ac resistance of multilayer transformer windings with arbitrary current waveforms," IEEE Trans. PE., vol. 15, Mar. 2000, pp. 369–376.

[4] M. E. Dale and C. R. Sullivan, "Comparison of Single-Layer and Multi-Layer Windings with Physical Constraints or Strong Harmonics", IEEE Int. Symp. on Industrial Electronics, Montreal, Que., Canada, July 2006, pp. 1467–1473.

[5] R. Severns, "Additional losses in high frequency magnetics due to non ideal field distributions", APEC Boston MA, 23-27 Feb. 1992, pp. 333-338.

[6] A. Pokryvailo, "Losses in a Conducting Cylinder Carrying Periodic Nonsinusoidal Current", Proc. 2014 IEEE International Power Modulator and High Voltage Conf., Santa Fe, NM, 1-5 June 2014, pp. 245-248.

[7] L.R. Neiman and K.S. Demirchyan, "Theoretical foundations of electricity," vol. 2, Energia, Leningrad, 1967, 408pp.